Magnetization steps in the diluted Heisenberg layer materials $(CH_3NH_3)_2Mn_xCd_{1-x}Cl_4$: Equilibrium data at 0.6 K

A. Paduan-Filho, X. Gratens, V. Bindilatti,* and N. F. Oliveira, Jr.
Instituto de Física, Universidade de São Paulo, Caixa Postal 66.318, 05315-970 São Paulo-SP, Brazil

Yaacov Shapira†
Department of Physics and Astronomy, Tufts University, Medford, Massachusetts 02155, USA
(Received 3 February 2005; revised manuscript received 3 May 2005; published 8 August 2005)

The magnetization M of $(CH_3NH_3)_2Mn_xCd_{1-x}Cl_4$, with x from 0.025 up to 0.265, was measured at 0.6 K in a slowly varying magnetic field B up to 17 T. The exchange interaction in these strongly diluted planar magnetic materials is antiferromagnetic. The in-plane cation structure is well approximated by a square lattice. The observed qualitative features, listed in the order that they appear in increasing B, are as follows: a fast rise of M, starting at $B=0$; a magnetization plateau (plateau of "apparent saturation"); a large magnetization step (MST), attributed to nearest-neighbor (NN) pairs; a second magnetization plateau; another large MST from NN pairs; and a third plateau that is not completed below the highest available B. These features are expected from the NN cluster model presented in the preceding paper. The magnetic fields at the two MST's give $J_1/k_B = (-4.39 \pm 0.10)$ K for the NN exchange constant. This value is slightly lower than reported for the undiluted $(x=1)$ member of this series, $(CH_3NH_3)_2MnCl_4$. A smaller J_1 when $x \leqslant 0.265$ may be the result of an in-plane expansion with decreasing x, caused by the slightly larger Cd^{2+} ion compared to Mn^{2+}. Analysis of the initial rise of M at low B indicates the presence of weak interactions that are not included in the NN cluster model. This conclusion is consistent with the observation (to be reported later) of a weak exchange interaction with a neighbor that is more distant than a NN. The apparent saturation value M_s, at the first magnetization plateau, was determined for all seven samples. There is a fair agreement with the values expected from a random distribution of the Mn ions over all cation sites. The largest deviation is for samples with $x \geqslant 0.15$, where the measured M_s is somewhat higher. In the same samples the magnetization jump ΔM at the MST's from NN pairs is somewhat smaller than for a random Mn distribution. A proposed explanation of the discrepancies for $x \geqslant 0.15$ postulates that the probability that a cation site is occupied by a Mn^{2+} is lowered by the presence of other Mn^{2+} ions at one or more NN cation sites.

DOI: 10.1103/PhysRevB.72.064415 PACS number(s): 75.60.Ej, 75.50.Ee, 71.70.Gm, 75.10.Jm

I. INTRODUCTION

In recent years the magnetization-step (MST) method has emerged as a powerful experimental technique for studying diluted antiferromagnetic (AF) materials.[1] The early works, since 1984, focused on diluted magnetic semiconductors.[2] More recently, MST's have been used to study model systems of AF insulators that are strongly diluted with nonmagnetic ions. The concentration of magnetic ions in these materials is well below the percolation concentration, so that there is no long-range AF order at any temperature. One previous study was on the three-dimensional (3D) antiferromagnet MnF_2, strongly diluted with zinc.[3] The model Heisenberg AF chain TMMC [i.e., $(CH_3)_4NMnCl_3$], strongly diluted with Cd, was studied later.[4]

The present experimental paper is the first of several on MST's from the 2D Heisenberg antiferromagnet $(CH_3NH_3)_2MnCl_4$, after it has been strongly diluted with Cd. The data reported here were taken at temperatures $T \approx 0.6$ K, using a slowly varying magnetic field B up to 17 T. The results at this relatively high temperature are interpreted using the simplest theoretical model, presented in the preceding paper.[5] Experimental data at 15 mK,[6] and the more elaborate theoretical model needed for analyzing the fine structure observed at this much lower temperature,[7] will be published later.

The series of compounds $(C_nH_{2n+1}NH_3)_2MnCl_4$ are among the best examples of 2D Heisenberg antiferromagnets.[8,9] These compounds have a perovskite-type layer structure.[10] The Mn^{2+} ions are in planes that are well separated from each other by organic layers whose thickness increases with increasing n. The large separation between the planes containing the Mn^{2+} ions is responsible for the nearly ideal 2D magnetic behavior. Figure 1, adapted from Ref. 11, shows a schematic of the crystal structure of methyl-ammonium-manganese-chloride (MAMC), which is the first member $(n=1)$ of this series. The planes with the Mn^{2+} ions are well separated by layers consisting of planes of Cl^- ions and (CH_3NH_3) groups.

The tetragonal crystal structure in Fig. 1 is the high-temperature structure of MAMC. In each of the tetragonal planes the Mn^{2+} ions form a square lattice. As the material is cooled, a series of crystallographic phase transitions take place. They involve ordering of the (CH_3NH_3) groups, and deformations of the quadratic $(MnCl_4)^{2-}$ layers.[10–12] The latter deformations are often ignored in the analysis of the magnetic properties of MAMC, i.e., the Mn^{2+} ions are assumed to form a square lattice.

The nonmagnetic compound $(CH_3NH_3)_2CdCl_4$ (or MACC), with Cd instead of Mn, is structurally analogous to MAMC. Its crystal structure at high temperatures is tetrago-

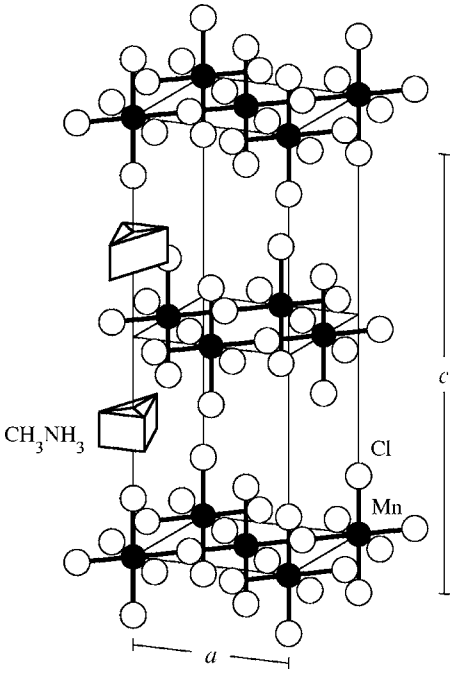

FIG. 1. Schematic of the crystal structure of $(CH_3NH_3)_2MnCl_4$. Adapted from Knorr *et al.* (Ref. 11). Unlike the notation in Ref. 5, *a* is one of the lattice constants of the tetragonal structure, not the distance between NN cations.

nal, similar to that in Fig. 1. When cooled it undergoes crystallographic phase transitions similar to those of MAMC.[12,13]

Early magnetic measurements by van Amstel and de Jongh[14] established that MAMC is a quasi-2D Heisenberg antiferromagnet. The Néel temperature is near 47 K, as was confirmed later.[15] The interlayer exchange coupling was estimated to be 8 or 9 orders of magnitude smaller than the intralayer exchange coupling. The anisotropy is 3 orders of magnitude smaller than the intralayer exchange, and is largely due to the dipole-dipole interaction.

An in-plane exchange constant $J/k_B=-5$ K was obtained by van Amstel and de Jongh from analysis of their susceptibility data. Reanalysis of the same data by Curély and Rouch[16] gave lower values, −3.6 and −3.8 K. However, the reliability of this later analysis is questionable (in our view) because it also gave a *g* factor for the Mn^{2+} ion that was well below the electron-paramagnetic-resonance (EPR) result $g=2.0045\pm0.0005$.[17] All values of *J* in the present paper are based on a convention in which the exchange interaction between spins $\mathbf{S}_1$ and $\mathbf{S}_2$ is given by

$$\mathcal{H}=-2J\mathbf{S}_1\cdot\mathbf{S}_2. \tag{1}$$

The exchange constant *J* was also obtained from the spin-wave spectrum, measured by inelastic neutron scattering.[18] The results were $J/k_B=-4.80$ K from "simple spin wave theory," and −4.69 K from "renormalized spin-wave theory." This *J* was identified as the nearest-neighbor (NN) in-plane exchange constant J_1. No influence of the next-nearest-neighbor exchange constant, J_2, on the spin-wave spectrum was detected.

The second-largest in-plane exchange constant, $J^{(2)}$ in the notation of Ref. 5, was measured only recently in our study of the MST's at 15 mK. This study will be published later.[6] The magnitude of $J^{(2)}$ is about 5% of the NN exchange constant J_1. At the temperatures of the experiments reported in the present paper, $T\approx0.60$ K, the fine structure caused by $J^{(2)}$ could not be resolved. For this reason, an adequate interpretation of the data reported here can be given using the NN cluster model, in which only J_1 is included.[5]

Several compositions of $(CH_3NH_3)_2Mn_xCd_{1-x}Cl_4$, with different values of *x*, were used in the present work. Obviously, these materials are intermediate between MAMC and its non-magnetic analog MACC. The Mn^{2+} ions occupy only a fraction *x* of the cation sites. The MST method of determining the NN exchange constant J_1 is most effective when *x* is well below the percolation concentration, $x_c=0.593$ for the NN cluster model.[19] For $x\ll x_c$, a sizeable percentage of the spins are in pairs composed of two Mn^{2+} ions that are NN's. Among all the series of MST's, those from NN pairs are by far the most useful for determining J_1.

II. THEORY

A. J_1 model

The J_1 model, presented in the preceding paper,[5] ignores all interactions other than the NN exchange and the Zeeman energy. This model is useful when (1) the NN exchange constant J_1 (assumed to be AF) is by far the largest, and (2) all anisotropies are small compared to the exchange interaction. In addition, k_BT (where k_B is the Boltzmann constant) must be small compared to J_1 but large compared to the other (neglected) exchange constants. The results quoted in Sec. I indicate that these minimum requirements for using the NN cluster model are satisfied by $(CH_3NH_3)_2Mn_xCd_{1-x}Cl_4$ at $T\approx0.60$ K. As described later, the main features of the data do follow from the J_1 model. However, some details of the magnetization curve require consideration of weak interactions that are neglected in this model.

The neglected weak interactions were discussed in Sec. VII of Ref. 1. They include exchange interactions with distant neighbors, anisotropies, and local strains[20] caused by the difference between the ionic radii of Mn^{2+} and Cd^{2+}.[21] The main effects produced by these weak interactions are as follows: (1) a broadening of the MST's, in addition to the thermal broadening which is included in the J_1 model; (2) a slower rise of the magnetization *M* at low magnetic fields, and (3) small shifts of the magnetic fields B_n at the MST's. The latter shifts must be considered in the determination of J_1.

Still other deviations from the predictions of the NN cluster model arise if the distribution of the magnetic ions over the cation sites deviates from the random distribution assumed in the model. Such deviations will affect the proportions of different features of the magnetization curve. This topic is discussed later.

B. Main features of the predicted magnetization curve

The main qualitative features of the magnetization curve at low *T*, in the order that they appear as *B* increases, are as

follows: (1) a fast rise of M at low B; (2) a plateau[22] at which M is equal to the apparent saturation value M_s; (3) several series of MST's, with plateaus between individual MST's; (4) finally, M reaches its true saturation value, M_0, after all the MST's are completed.

Each series of MST's originates from one of the cluster types that are discussed in Ref. 5. The only cluster type that does not give rise to MST's is the "single," i.e., a magnetic ion with no NN's. For low x, the largest MST's are from NN pairs.

The apparent saturation value M_s is the magnitude of the magnetization rise at low B. The main contribution to M_s is from the singles.[1] The magnetization jump ΔM at any of the MST's originating from NN pairs is proportional to the number (or "population") of NN pairs. More generally, the jump ΔM at any MST originating from a given cluster type is proportional to the number of clusters of that type.

C. Obtaining J_1 from MST data

NN pairs, composed of two ions of spin S, give rise to a series of $2S$ MST's. In the "pure" J_1 model, the magnetic field B_n at the nth MST is given by[1]

$$g\mu_B B_n = 2n|J_1|. \tag{2}$$

In this simple model, any of the fields B_n can be used to determine J_1. In reality, however, the weak interactions that are neglected in the pure J_1 model result in small deviations from Eq. (2). It is then preferable to determine J_1 from the difference between the fields at successive MST's. That is,

$$g\mu_B(B_{n+1} - B_n) = 2|J_1|. \tag{3}$$

Equation (3) was originally obtained by Larson *et al.*[23] Although this equation is based on an approximation, it has been quite successful. Usually the accuracy for J_1 achieved with this equation has been better than 2% (see Ref. 1).

D. Nonrandom distribution of magnetic ions

The populations of various cluster types depend on the distribution of the magnetic ions over the cation sites. The theory in Ref. 5 was based on the usual assumption that the distribution is random. That is, the probability that any cation site is occupied by a magnetic ion (here, Mn^{2+}) is always equal to the fraction x of cations that are magnetic.

The assumption of a random distribution is crucial: the calculated magnitudes of M_s, and of the magnetization jump ΔM at each of the MST's, are based on this assumption. However, the validity of Eq. (3), and therefore also of the value of J_1 obtained by using it, is independent of the manner in which the Mn ions are distributed over the cation sites. Empirically, magnetization curves for many diluted magnetic materials, particularly those grown from the melt at high temperatures, agreed with a random distribution. However, deviations from a random distribution were found in some cases.[1]

A detailed characterization of a nonrandom distribution of two species of cations (here, Mn^{2+} and Cd^{2+}) over the cation sites is beyond the scope of this work. In what follows, some ideas that will be used in the data interpretation are presented. Three types of deviations from a random distribution, associated with different length scales (short, intermediate, and long), are considered. The three types are not mutually exclusive; more than one type may exist in the same material.

1. Short-range correlations

The probability that a cation site is occupied by a Mn ion may depend on the presence of other Mn ions on neighboring cation sites, at distances comparable to the lattice constant a. The distribution of the Mn ions on this length scale governs the distribution of chemical bonds in the material. It also governs the distribution of local strains[20] caused by the different ionic radii[21] of Mn^{2+} and Cd^{2+}. The energies associated with chemical bonds and with local strains therefore depend on the manner in which Mn ions are distributed over distances of order a. A nonrandom distribution, with short-range correlations between the locations of the Mn ions, may be preferred energetically.

The actual short-range correlations are not governed only by the energy. The entropy term in the free energy, which favors a random distribution, also plays a role. Because the entropy term increases with increasing T, the growth temperature of the sample may influence the short-range correlations. The ability of the Mn ions to redistribute themselves by diffusion, after the sample is grown, may also be a factor.

One type of short-range correlation is a nearest-neighbor site correlation (NNSC). For a random distribution the probability P_{occup} that a cation site is occupied by a Mn ion is always equal to x, regardless of the locations of other Mn ions. When NNSC exists, P_{occup} depends on the presence of one or more Mn ions on NN cation sites. The NNSC will be considered to be positive if the presence of one or more Mn ions on NN sites causes P_{occup} to be larger than x, and negative if $P_{\text{occup}} < x$.

Consider a sample with a fixed number of Mn ions. A negative NNSC increases the population of singles, because there is a lower probability that any of the NN cation sites surrounding a Mn ion is occupied by another Mn ion. Because the total number of Mn ions is constant, the population of at least one cluster type that is not a single (NN pairs, NN triplets, etc.) will decrease. The experimental consequence of a larger number of singles is a larger magnetization rise at low fields, i.e., a larger M_s than expected from a random distribution. The decrease in the populations of one or more of the larger cluster types (NN pairs, NN triplets, etc) will lead to smaller magnetization jumps, ΔM, at the MST's from these cluster types. For some of the samples studied in the present work, the results for M_s, and for ΔM from NN pairs, are consistent with these predictions for a negative NNSC. In an earlier study of quasi-2D heterostructures, the observed ΔM from NN pairs was smaller than predicted from a random distribtution.[24] However, the possibility that this discrepancy was due to a negative NNSC was not discussed.

The opposite effects will result from a positive NNSC. The population of the singles will decrease, so that the observed M_s will be smaller than for a random distribution. At the same time, the population of at least one cluster type that

TABLE I. Mn concentration x for the various products. The results are (1) from susceptibility data and (2) from the ratio of the Mn and Cd concentrations obtained by chemical analysis (ICP-AES). The ICP-AES value in parenthesis is from the Mn concentration alone, assuming the nominal composition $(CH_3NH_3)_2Mn_xCd_{1-x}Cl_4$. The last column gives the "chosen value" (average over all measured values for the product), and the uncertainty (standard deviation).

Product	x (Susceptibility)	x (ICP-AES)	x (chosen value)
A	0.033; 0.0175		0.025±0.011
B	0.053	0.074 (0.074); 0.061 (0.061)	0.063±0.011
C	0.075; 0.067	0.060(0.0585)	0.067±0.008
D	0.070; 0.080; 0.085		0.078±0.008
E	0.15; 0.165	0.150(0.152); 0.161(0.160)	0.157±0.008
F	0.170; 0.174		0.172±0.003
G	0.25; 0.28		0.265±0.021

gives rise to MST's will increase, causing the magnetization jumps ΔM at the MST's from this cluster type to be larger.

2. Segregation into high and low concentration regions

Another cause of a nonrandom distribution is segregation: the magnetic ions are segregated into high- and low-concentration regions of "intermediate size." A region of intermediate size has a volume (area for a true 2D material) that is large enough for a meaningful definition of a concentration, but is orders of magnitude smaller than the volume of the entire sample. For example, in bulk samples with $10^{19}-10^{22}$ cation sites, volumes that contain, say, 10^6-10^9 cations are of intermediate size.

Experimental evidence for a nonrandom distribution due to segregation was reported for some DMS samples containing Eu^{2+} ions.[25,26] A model which probably oversimplifies the actual situation was used to interpret these results.[1] In this model all the magnetic ions are in "occupied regions," while all other regions are totally devoid of magnetic ions. The magnetic ion concentration in the occupied regions is defined as the "local concentration," x_L. In the absence of segregation, $x_L=x$. When segregation exists, x_L is higher than the average concentration x for the sample as a whole. The ratio x_L/x is a measure of the degree of segregation.

A major assumption of the model is that within the occupied regions, the distribution of magnetic ions is random. The probability that a magnetic ion in the occupied regions belongs to a particular cluster type (single, NN pair, NN triplet, etc.) is calculated assuming that the distribution of magnetic ions in the occupied regions is random, but with a concentration that is equal to x_L instead of x. When segregation is present $x_L>x$, the singles' population is reduced, resulting in a lower ratio M_s/M_0 compared to that calculated from a random distribution over the sample a whole. At the same time, the population of at least one of the cluster types that give rise to MST's must increase. The increased population increases the size ΔM of the MST's associated with the relevant cluster type (or types). A lower ratio M_s/M_0, compared to that from a random distribution over the sample as a whole, was observed clearly in $Sn_{1-x}Eu_xTe$.[1,26] At the same time, the sizes of the MST's from both NN pairs and NN triplets were larger than predicted. The interpretation of these results in terms of segregation[27] was supported by the observation of the magnetic signature of antiferromagnetic EuTe precipitates in similarly-grown samples.[28]

In the simple model that was just outlined, the qualitative effects of segregation on the magnetization curve are similar to those resulting from a positive NNSC. In both cases, M_s/M_0 is lower, and at least some of the MST's are accompanied by larger magnetization jumps ΔM. This similarity is expected. In the simple model for segregation, any Mn ion must be in an "occupied region." All the NN cation sites surrounding this ion are also in the same occupied region.[29] Therefore, the probability P_{occup} that an NN cation site is occupied is x_L. Because x_L is larger than x, the NNSC is positive.

3. Long-range concentration gradients

A gradual variation of x, on a macroscopic length scale comparable to the sample size, is quite common. Often, the variation is moderate in size, say, $\Delta x/x<0.3$. By themselves, such moderate long-range concentration gradients do not produce major changes in the magnetization curve. In the absence of other causes of nonrandomness, the magnetization curve remains close to that calculated for a random distribution using the average concentration for the sample as a whole. Physically, the effects of long-range concentration gradients tend to average out.

III. EXPERIMENT

A. Sample preparation

Single-crystal platelets of $(CH_3NH_3)_2Mn_xCd_{1-x}Cl_4$ were obtained from solutions of methyl-ammonium-chloride, manganese chloride, and cadmium chloride, in ethanol. Seven such solutions were evaporated at 30 °C. The platelets obtained from a single solution are called the "product" of the solution. The total mass of a product varied between 0.1 and 0.4 g. A large solution volume, typically 300 ml, helped to maintain a constant Mn concentration in the solution, and hence in the product. The Mn concentrations x in the products were all below 0.27.

The single-crystal platelets had typical dimensions of $3\times3\times1$ mm. Their color changed gradually from pink to

white as the Mn concentration decreased. A fine powder was obtained from each product by grinding. The products from the seven solutions are labeled as A, B, C, D, E, F, and G. Only a portion of the fine powder from each of the products was used in measurements of the MST's at $T \approx 0.60$ K. The portion that was used is called the "MST sample." Each MST sample is labeled by the letter, from A to G, which was assigned to the product.

B. Mn concentration

The Mn concentration x was determined by two methods: (1) from the Curie constant, obtained from the temperature variation of the low-field magnetic susceptibility χ, and (2) by chemical analysis.[30] These measurements were made on two or more portions of each of the seven products. At least one of these portions was taken from the MST sample.

The susceptibility data were obtained with two magnetometer systems equipped with superconducting quantum interference devices (SQUID's).[31] The magnetic fields B ranged from 0.05 to 0.5 T. Data in the range $150\ \mathrm{K} \leqslant T \leqslant 300$ K were fitted to the Curie-Weiss law. In each fit the diamagnetic susceptibility χ_d, from all sources other than the Mn spins, was treated as the third adjustable parameter (in addition to the Curie constant and Curie-Weiss temperature). The Mn concentration x was calculated from the Curie constant per unit mass assuming the nominal composition, $(CH_3NH_3)_2Mn_xCd_{1-x}Cl_4$. The values $S=5/2$ and $g=2.00$ were used for the Mn^{2+} ion.

The chemical analysis determined both the Mn and Cd concentrations, expressed in weight percent. Atomic emission spectroscopy with inductively-coupled plasma (ICP-AES) was used. The value of x was calculated from the ratio between the Mn and Cd concentrations. Another value for x was obtained from the concentration of Mn alone, assuming the nominal composition.

Values of x obtained for different portions of the same product showed some variation. At least for some products the variation was larger than the measurement accuracy, indicating the presence of macroscopic concentration gradients. The largest percentage variation of x was in product A, with the lowest x. It is safe to assume that concentration gradients existed in each of the MST samples.

Table I lists the results for x, obtained on different portions of each of the seven products. The ICP-AES value is based on the ratio of the Mn and Cd concentrations. The ICP-AES value from the Mn wt % alone is shown in parenthesis. The "chosen value," given in the last column, is the average of all measured values of x for the product. The quoted uncertainty is the standard deviation.

A complete chemical analysis was carried out only in one case, on a portion of product C. This is the portion for which the susceptibility gave $x=0.067$. Three parts of that portion were analyzed. Elemental analysis of one part gave the following concentrations (in wt%): carbon 8.2, nitrogen 8.7, hydrogen 3.35. The values expected from the chemical formula are 7.6, 8.9, and 3.85, respectively. The second part of that product was analyzed for chlorine. The result was 43.9 wt %, compared to the expected value 45.1 wt %. ICP-AES analysis of the third part gave $x=0.060$ from the ratio of the Mn and Cd concentrations, and 0.0585 from the Mn concentration alone.

C. Magnetization measurements

The magnetization M of the MST samples was measured at temperatures $T \approx 0.60$ K in magnetic fields B up to 17 T. A vibrating sample magnetometer (VSM) was used. Each powder sample, with a typical mass of 70 mg, was immersed in a liquid ^{3}He bath, contained in an insert Dewar.[32] Temperatures from 0.55 to 0.65 K were obtained by pumping on the ^{3}He bath. The magnetic field was produced by a superconducting magnet. The one-way sweep time (up to the maximum field, or back to zero) was about 50 min. At this sweep rate, hysteresis was not observed in most samples. In the few cases that hysteresis was present, it was very small and was confined to the low-field region where M varied rapidly with B. There was no hysteresis near the MST's.

The magnetization curves shown below are averages of up and down field sweeps. These results were corrected for the diamagnetic contribution from orbital motion in the sample, and for the addenda. The correction increased monotonically with B. At the highest B, the correction for sample A (the lowest x) reached 4%. For sample G (highest x) it was less than 1%.

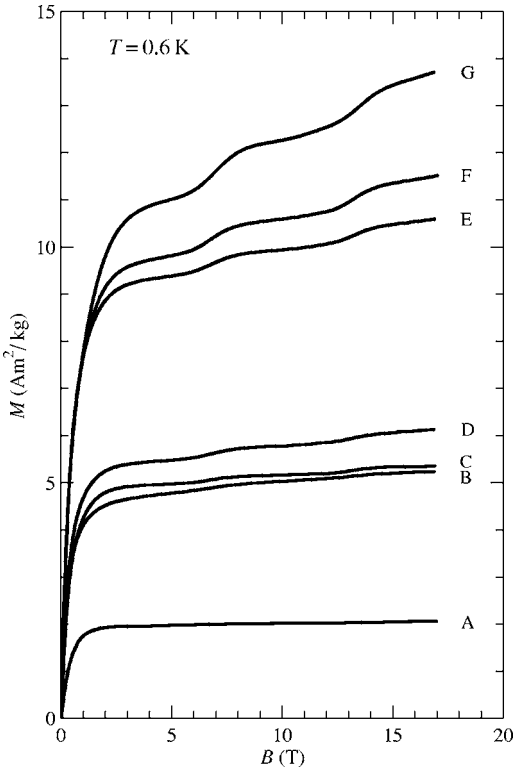

FIG. 2. Magnetization curves for the seven MST samples at $T \approx 0.60$ K. The "chosen values" of x (Table I) are 0.025 for sample A, 0.063 for B, 0.067 for C, 0.078 for D, 0.157 for E, 0.172 for F, and 0.265 for G. The SI unit Am^2/kg for the ordinate scale is equivalent to emu/g.

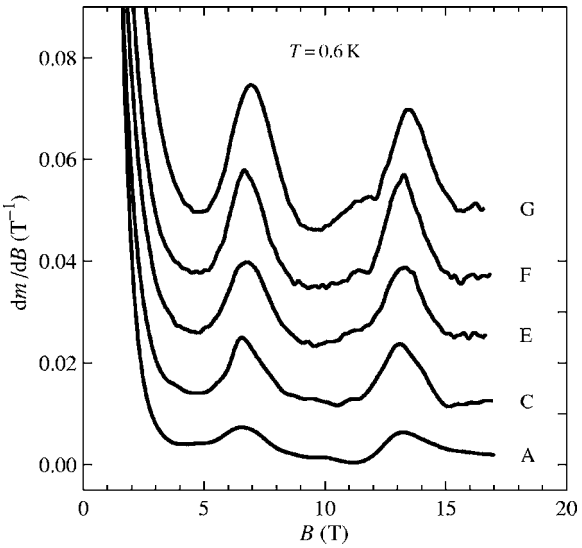

FIG. 3. Magnetic field dependence of the derivative dm/dB of the normalized magnetization $m=M(B)/M(17\ \mathrm{T})$ for five of the samples. These results were obtained numerically from the curves in Fig. 2.

IV. RESULTS

A. Magnetization curves

The magnetization curves at $T\approx 0.60$ K for all seven MST samples are shown in Fig. 2. The main features of all the magnetization curves are as follows: a fast rise at low fields; two MST's at higher magnetic fields; and "plateaus" (slow variation of M) before and after each MST. These features are expected from the NN cluster model.[5] The first plateau, after the fast rise at low B but before the first MST, is the plateau of apparent saturation. The value of M at this plateau is the apparent saturation value M_s.

The two MST's are seen more clearly as peaks in the derivative dM/dB. For presentation purposes, it is convenient to show the derivative of the normalized magnetization $m=M(B)/M(17\ \mathrm{T})$, where $M(17\ \mathrm{T})$ is the magnetization at the highest available field in these experiments (see Ref. 33 for a comment on the notation). Figure 3 shows the field variation of dm/dB for five of the samples. These curves were obtained by numerical differentiation of the data in Fig. 2. The derivative curves for the other two samples, B and D, are similar.

B. NN exchange constant

The fields at the maxima of the derivative peaks were chosen as the fields B_1 and B_2 at the first and second MST's. Table II gives their values for all samples. The difference B_2-B_1 is also given. The average and standard deviation for (B_2-B_1) are 6.520 ± 0.067 T. Including the uncertainty in the field calibration, the estimated uncertainty for (B_2-B_1) is 0.15 T. Using Eq. (3) and $g=2.0045$,[17] the results for (B_2-B_1), give $J_1/k_B=(-4.39\pm0.10)$ K.

For pure MAMC ($x=1$) the best values for J_1/k_B are probably from the two analyses of inelastic neutron scattering data, i.e., -4.69 K and -4.80 K.[18] The slightly lower value obtained in the present work is for $x<0.3$. The difference is apparently due to a decrease of J_1 with decreasing x. That is, J_1 decreases as more Mn^{2+} ions are replaced by Cd^{2+}. The dominant superexchange bond between two nearest-neighbor Mn^{2+} ions is presumably through the intervening Cl^- ion (see Fig. 1). Structural data, such as those in Refs. 11 and 13, indicate that this bond is about 3% shorter for $x=1$ (MAMC) than for $x=0$ (MACC). The shorter bond is consistent with the smaller ionic radius of Mn^{2+}, compared to that of Cd^{2+} (Ref. 21). Exchange constants usually increase as the bond becomes shorter. Therefore, J_1 is expected to increase with increasing x. Table II gives no indication of such an increase, but the range of x in this table is rather limited. The expected variation of J_1 in this range is only slightly larger than the standard deviation.

An additional reason for the slightly smaller J_1 obtained in the present work are the different methods of data analysis. In the analyses of the neutron-scattering data,[18] only the exchange constant J_1 was included. As will be reported later,[6] the second-largest exchange constant, $J^{(2)}$, is about 5% of J_1. In the present work J_1 was extracted from the MST data using Eq. (3). This equation includes the correction for $J^{(2)}$ suggested in Ref. 23.

V. COMPARISON WITH SIMULATIONS

A. Simulations

All simulations in this paper are based on the NN cluster model (J_1 model), presented in the preceding paper.[5] Only one exchange constant, $J_1/k_B=-4.39$ K, is included. Simulations which also include $J^{(2)}$ will be presented later.[6] The simulations treat exactly clusters containing up to 5 NN spins. Larger clusters are treated using the rise-and-ramp ap-

TABLE II. Values of B_1 and B_2 at the two observed peaks in dm/dB, and the difference B_2-B_1.

Sample	x	B_1(T)	B_2(T)	B_2-B_1(T)
A	0.025	6.56	13.20	6.64
B	0.063	6.68	13.10	6.42
C	0.067	6.58	13.11	6.53
D	0.078	6.65	13.12	6.47
E	0.157	6.78	13.31	6.53
F	0.172	6.74	13.27	6.53
G	0.265	6.95	13.47	6.52

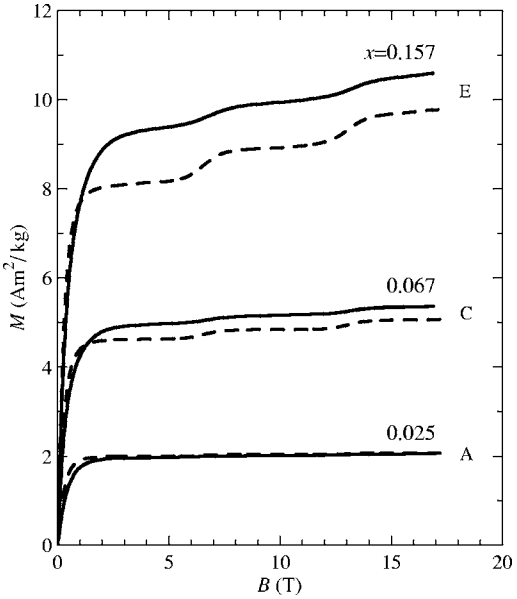

FIG. 4. Measured magnetization curves (solid lines) and the corresponding simulated magnetization curves (dashed lines) for samples A (x=0.025), C (x=0.067), and E (x=0.157). The simulations use the NN cluster model at the actual experimental temperature, T=0.6 K.

proximation. This approximation becomes less accurate as x increases. For the six MST samples with $x<0.20$ the estimated accuracy for M, at all values of B, is better than about 1%. For sample G, with x=0.265, nearly 23% of the spins are treated only approximately, compared to 9.4% for x =0.20. The accuracy for sample G may therefore be worse than 1%, except for the value of the apparent saturation value M_s. In the calculation of M_s, clusters with up to 12 spins (instead of up to 5 spins) are treated exactly.[5] The accuracy

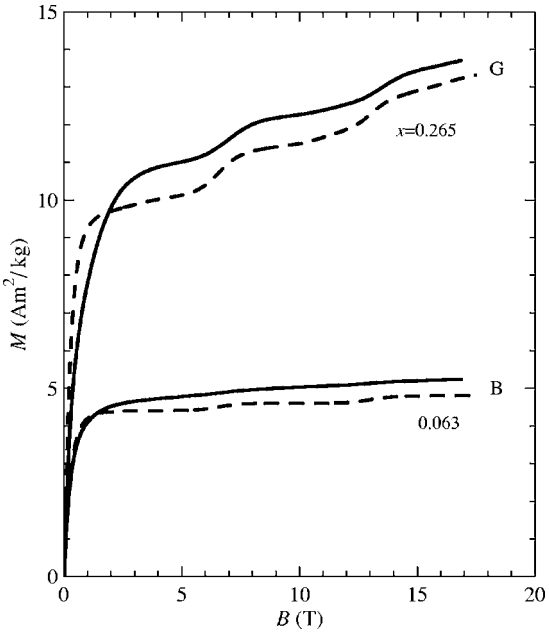

FIG. 5. The measured (solid) and simulated (dashed) magnetization curves for samples B (x=0.063)) and G (x=0.265)).

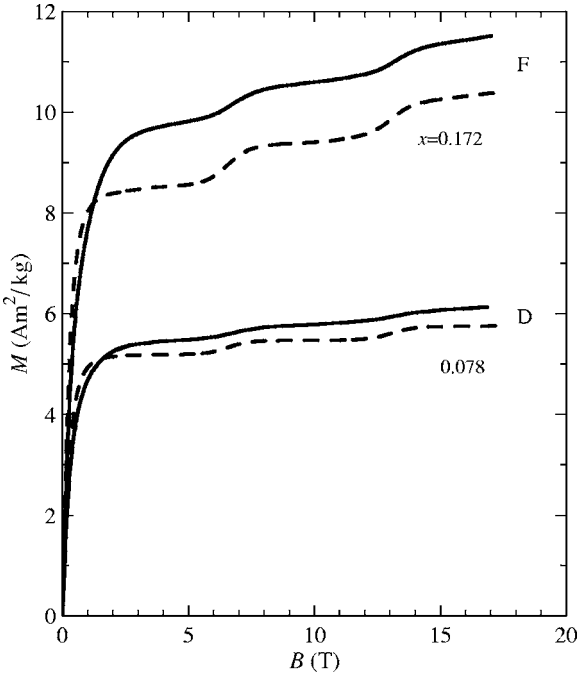

FIG. 6. The measured (solid) and simulated (dashed) magnetization curves for samples D (x=0.078) and F (x=0.172).

for M_s is therefore higher. For all seven samples in the present work, including G, the expected accuracy of the calculated M_s is better than 1%.

In comparing the simulations with the experimental curves, the following points should be kept in mind: (1) The simulations assume a random Mn distribution over all the cation sites. As noted in Sec. II D, a failure of this assumption can lead to significant discrepancies with experimental values for M_s and ΔM. (2) For each sample, the simulation is for the "chosen value" of x, given in Table I. The true average concentration for the sample may be slightly different, as indicated by uncertainty quoted in this table. (3) In the simulations, thermal broadening is the only broadening mechanism for the MST's and for the magnetization rise at low B. This thermal broadening was calculated for the actual temperature, T=0.6 K. Non-thermal broadening mechanisms that were discussed in Refs. 1 and 20 include exchange interactions with distant neighbors, various anisotropies, and local strains due to the different ionic sizes of Mn^{2+} and Cd^{2+}.

B. Measured and simulated magnetization curves

Measured and simulated magnetization curves for all the MST samples are compared in Figs. 4–6. (Three figures are used, in order to clearly separate the results for the seven samples.) There are no adjustable parameters in the simulations. The overall agreement between the simulations and the data is satisfactory, but there are some discrepancies.

The comparison between the measured and simulated magnetization curves will be divided into three topics: (1) the rapid rise of M at low fields; (2) the apparent saturation plateau, and the apparent saturation value M_s; (3) the two MST's from NN pairs.

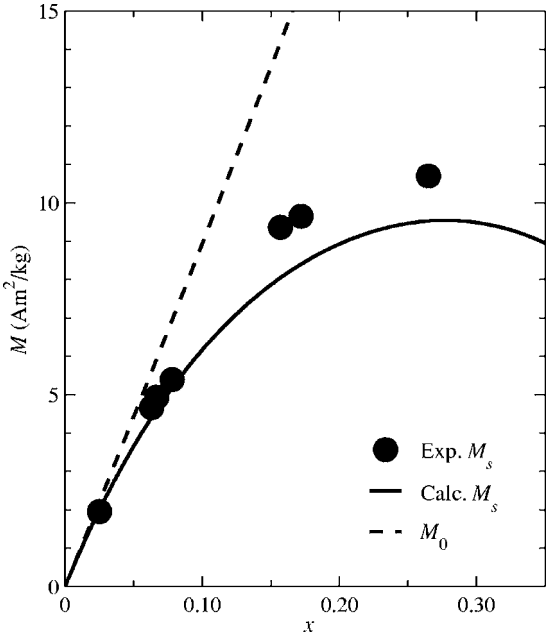

FIG. 7. Apparent saturation value M_s as a function of x. The filled circles are the experimental values for the various samples, expressed in Am^2/kg (equivalent to emu/g). The solid curve is the calculated M_s, assuming a random Mn distribution. The dashed curve is the saturation magnetization M_0.

1. Fast magnetization rise at low fields

The fast rise in low magnetic fields ends with a smooth transition to the plateau of apparent magnetic saturation. The results in Figs. 4–6 indicate that the observed smooth transition occurs at somewhat higher fields than in the simulations. It will be shown in a later paper[6] that this discrepancy is mainly due to the neglect, in the simulations, of the second-largest exchange constant, $J^{(2)}$. The additional AF exchange interaction associated with $J^{(2)}$ slows the alignment of the spins at low fields. The plateau of apparent saturation does not begin until the Zeeman energy is large enough to saturate the magnetic moments of most clusters that involve only $J^{(2)}$ exchange bonds.

2. Plateau of apparent saturation

All samples show the plateau of apparent saturation. For sample G, with the highest x, there is a noticeable increase of M in the plateau, both experimentally and in the simulations (Fig. 5). This increase is mainly due to the first MST from the so-called string quartets (cluster type 4*A* in Ref. 5). The simulation in Fig. 10 of Ref. 5 shows that the first MST from 4*A* quartets is near the middle of the plateau of apparent saturation. The size ΔM of the magnetization jump at this MST depends on x, and is significant when x reaches the value 0.265 for sample G. Although the first MST from 4*A* quartets was not resolved in the experiment, it did affect the plateau.

Figure 7 shows the experimental values of M_s as a function of x. These results are expressed in Am^2/kg. (In contrast to Fig. 12 of Ref. 5, the apparent saturation value M_s is not normalized to the true saturation value M_0.) The solid curve in Fig. 7 is the calculated M_s for a random Mn distribution over all cation sites. It represents the prediction of the model used in the simulations. The dashed curve gives the calculated true saturation magnetization M_0, i.e., when all the spins are parallel. Obviously, measured values of M_s can never exceed M_0, regardless of the distribution of the Mn ions over the cation sites.

The experimental points in Fig. 7 are in fair agreement with a random distribution (solid curve). The very good agreement for sample A (lowest x) may not be significant in view of the relatively large uncertainly in x (Table I). For the other three samples with $x<0.1$ the experimental points are only slightly above the solid curve. However, for the three samples with $x\geqslant 0.15$ the discrepancy, although not huge, is quite obvious. It is also obvious in Figs. 4–6 (samples E, F, and G). The percentage discrepancy is largest for sample E, with x near 0.16. For this sample the observed M_s is 16% higher than for a random distribution. A possible cause for the discrepancy will be discussed later.

3. MST's from NN pairs

The comparison between the observed and simulated MST's focused on the size ΔM of the magnetization jump. For $x<0.1$, the experimental precision for ΔM was low because $\Delta M \ll M_s$, and because in some samples (e.g., sample D) the baseline for measuring ΔM was uncertain due to significant rounding of the MST's. The only conclusion reached for $x<0.1$ is that there is no obvious discrepancy between the observed and simulated values of ΔM.

For two of the three samples with $x\geqslant 0.15$ the observed ΔM is definitely smaller than in the simulations. For sample E (Fig. 4) the observed ΔM is about 25% smaller than in the simulation. The discrepancy for sample G (Fig. 5) is less obvious because of the larger monotonic increase of M on which the MST's are superimposed. A rough estimate for sample G, from expanded plots of the top parts of the measured and simulated curves (not shown), is that the observed ΔM is 15% smaller than in the simulation. The smaller-than-predicted sizes of the observed ΔM imply that the actual populations of NN pairs in samples E and G are lower than for a random Mn distribution. It is surprising that for sample F, with x not very different from that for sample E, the discrepancy in ΔM is only about 10%. The reason why the discrepancies in ΔM for samples E and F are not comparable is not known. The discrepancies in M_s (Fig. 7) are comparable.

4. Discussion of the discrepancies in M_s and ΔM

The discrepancies in both M_s and ΔM are most conspicuous for $x\geqslant 0.15$. The observed M_s is noticeably larger. The observed ΔM for two of the samples is lower than for a random distribution of the Mn ions over all cation sites. A possible explanation of these discrepancies has already been discussed in Sec. II D 1. A nonrandom distribution due to a short-range correlation with a negative NNSC should lead to a higher M_s and a lower ΔM. The growth temperature of the present samples, 30 °C, is relatively low. A nonrandom distribution is therefore more likely than in the II-VI diluted

magnetic semiconductors (DMS's) that were studied earlier.[1,2] These DMS's were grown from the melt at much higher temperatures.

An alternative explanation of the discrepancy in M_s initially seemed to be promising, but was ultimately viewed as unlikely. It assumed the presence of an "impurity phase." That is, a small portion of the sample has different chemical composition and crystal structure than the main portion, with the composition $(CH_3NH_3)_2Mn_xCd_{1-x}Cl_4$. Such an impurity phase was observed by van Amstel and de Jongh[14] in samples of MAMC. An example of an impurity, suggested by them, is the antiferromagnet $MnCl_2.4H_2O$. It has a Néel temperature $T_N=1.6$ K, and a saturation field of about 2 T (Ref. 34). Because M_s was determined in fields above 2 T, the full saturation moment of the impurity phase would have contributed to the measured M_s.

There were two reasons why the impurity-phase scenario was ultimately regarded as very unlikely. First, for some samples the required fraction of Mn ions in the impurity phase was quite large. For sample E, with the largest discrepancy in M_s, about 20% of the Mn ions were required to be in the impurity phase. This is an unreasonably large fraction, in our view. The second reason was that ac susceptibility data for sample F, with the second-largest discrepancy in M_s, showed no sign of an antiferromagnetic transition at 1.6 K.

VI. CONCLUSION

The NN cluster model gives a satisfactory account of the main features of the experimental data. Among the details that deviate from the model, some will be explained by the second-largest exchange constant $J^{(2)}$. Although small compared to J_1, this exchange constant is not negligible. The definite, but fairly small, discrepancies between observed and predicted values of M_s and ΔM may have been caused by a negative NNSC.

ACKNOWLEDGMENTS

This work was supported by the Brazilian agencies CNPq and FAPESP. Travel funds for Y.S. were provided by FAPESP.

*Electronic address: vbindilatti@if.usp.br
†Electronic address: yshapira@granite.tufts.edu

[1] Y. Shapira and V. Bindilatti, J. Appl. Phys. **92**, 4155 (2002).
[2] Y. Shapira, J. Appl. Phys. **67**, 5090 (1990).
[3] X. Gratens, V. Bindilatti, E. ter Haar, N. F. Oliveira, Jr., Y. Shapira, and F. C. Montenegro, Phys. Rev. B **64**, 214424 (2001).
[4] A. Paduan-Filho, N. F. Oliveira, Jr., V. Bindilatti, S. Foner, and Y. Shapira, Phys. Rev. B **68**, 224417 (2003).
[5] V. Bindilatti and Y. Shapira, preceding paper, Phys. Rev. B **72**, 064414 (2005).
[6] X. Gratens *et al.* (unpublished).
[7] V. Bindilatti and Y. Shapira (unpublished).
[8] *Magnetic Properties of Layered Transition Metal Compounds*, edited by L. J. de Jongh (Klüwer, Dordrecht, 1989).
[9] L. J. de Jongh and A. R. Miedema, Adv. Phys. **23**, 1 (1974).
[10] R. Arendt, R. Hoffman, and F. Waldner, Solid State Commun. **13**, 1629 (1973); R. Kind and J. Roos, Phys. Rev. B **13**, 45 (1976).
[11] K. Knorr, I. R. Jahn, and G. Heger, Solid State Commun. **15**, 231 (1974).
[12] R. Kind, R. Blinc, and B. Zeks, Phys. Rev. B **19**, 3743 (1979).
[13] G. Chapuis, R. Kind, and H. Arendt, Phys. Status Solidi A **36**, 285 (1976).
[14] W. D. van Amstel and L. de Jongh, Solid State Commun. **11**, 1423 (1972).
[15] A. Paduan-Filho and C. C. Becerra, J. Appl. Phys. **91**, 8249 (2002).
[16] J. Curely and J. Rouch, Physica B **254**, 298 (1998); K. W. Lee, C. H. Lee, C. E. Lee, and J. K. Kang, Phys. Rev. B **62**, 95 (2000).
[17] H. B. Boesch and F. Waldner, in *Local Properties of Phase Transitions*, edited by K. A. Muller and A. Rigamonti (North-Holland, Amsterdam, 1976), p. 642 ff.
[18] B. Schroder, V. Wagner, N. Lehner, K. M. Kesharwani, and R. Geick, Phys. Status Solidi B **97**, 501 (1980).
[19] D. Stauffer and A. Aharony, *Introduction to Percolation Theory*, revised 2d ed. (Taylor & Francis, London, 1994).
[20] Y. G. Rubo, M. F. Thorpe, and N. Mousseau, Phys. Rev. B **56**, 13094 (1997).
[21] R. D. Shannon, Acta Crystallogr., Sect. A: Cryst. Phys., Diffr., Theor. Gen. Crystallogr. **32**, 751 (1976); R. D. Shannon and C. T. Prewitt, Acta Crystallogr., Sect. B: Struct. Crystallogr. Cryst. Chem. **25**, 925 (1969); **26**, 1046 (1970).
[22] The term "plateau" does not mean the total absence of any variation of M with B. It only means that the variation is very slow.
[23] B. E. Larson, K. C. Hass, and R. L. Aggarwal, Phys. Rev. B **33**, 1789 (1986).
[24] S. A. Crooker, N. Samarth, and D. D. Awschalom, Phys. Rev. B **61**, 1736 (2000).
[25] E. terHaar, V. Bindilatti, N. F. Oliveira, Jr., G. H. McCabe, Y. Shapira, Z. Golacki, S. Charar, M. Averous, and E. J. McNiff, Jr., Phys. Rev. B **56**, 8912 (1997).
[26] X. Gratens, E. ter Haar, V. Bindilatti, N. F. Oliveira, Jr., Y. Shapira, M. Liu, Z. Golacki, S. Charar, and A. Errebbahi, J. Phys.: Condens. Matter **12**, 3711 (2000).
[27] The term "segregation" was not used explicitly in the earlier work on $Sn_{1-x}Eu_xTe$.
[28] M. Gorska, J. R. Anderson, J. L. Peng, and Z. Golacki, J. Phys. Chem. Solids **56**, 1253 (1995); J. R. Anderson, M. Gorska, Y. Oka, J. Y. Jen, I. Mogi, and Z. Golacki, Solid State Commun. **96**, 11 (1995).
[29] The number of spins that are just on the border of an occupied region of intermediate size is negligible compared to the number of spins inside the region.
[30] Chemical analysis was performed at Central Analítica - Instituto de Química, Universidade de São Paulo.
[31] One system was manufactured by Quantum Design, Inc., San Diego, CA, and the other by Cryogenics Ltd., London, England.

[32] N. F. Oliveira, Jr. and S. Foner, Rev. Sci. Instrum. **43**, 37 (1972).
[33] In Ref. 5, $m=M/M_0$ is the value of M normalized to the true saturation value M_0. In the present work, the maximum available maximum field, 17 T, was insufficient for reaching true saturation. Therefore, M was normalized to $M(17\ \mathrm{T})$.
[34] J. E. Rives and V. Benedict, Phys. Rev. B **12**, 1908 (1975).